ISSN 0022-4766, Journal of Structural Chemistry, 2019, Vol. 60, No. 5, pp. 789-795. © Pleiades Publishing, Inc., 2019.
Russian Text © The Author(s), 2019, published in Zhurnal Strukturnoi Khimii, 2019, Vol. 60, No. 5, pp. 823-829.

A STUDY OF THE CRYSTAL STRUCTURE OF $SmCaCo_{1-x}Fe_xO_{4-\delta}$ AND $Sm_{0.9}Ca_{1.1}Fe_{1-y}Co_yO_{4-\delta}$ SOLID SOLUTIONS

A. P. Galayda, N. E. Volkova, A. A. Startseva, L. Ya. Gavrilova, and V. A. Cherepanov

Complex oxides with general compositions $SmCaCo_{1-x}Fe_xO_{4-\delta}$ and $Sm_{0.9}Ca_{1.1}Fe_{1-y}Co_yO_{4-\delta}$ are synthesized using the glycerol-nitrate technique at 1100 °C in air. By powder X-ray diffraction it is determined that $SmCaCo_{1-x}Fe_xO_{4-\delta}$ solid solutions exist in a composition range $0 \le x \le 0.3$ and $Sm_{0.9}Ca_{1.1}Fe_{1-y}Co_yO_{4-\delta}$ solid solutions exist in a composition range $0 \le y \le 0.7$. The samples with high concentrations of cobalt ions are found to crystallize in the tetragonal unit cell (space group *I*4/*mmm*), whereas the solid solutions enriched with iron ions have the orthorhombic structure (space group *Bmab*). For all single phase samples the unit cell parameters and volume and the structural parameters (atomic coordinates and bond lengths) are calculated by the full-profile Rietveld method.

DOI: 10.1134/S0022476619050111

Keywords: complex oxides, Ruddlesden–Popper phases, ferrites, cobaltites, powder X-ray diffraction analysis, crystal structure.

INTRODUCTION

Oxide materials based on rare earth elements and 3*d* transition metals are now broadly used in the design of many electrochemical devices, such as high and intermediate temperature fuel cells, oxygen membranes, semiconductor gas sensors [1-6]. The research interest in these compounds stems from a set of their physicochemical properties (high electron and ion conductivity, stability in an oxidizing environment, thermal stability in a broad temperature range) largely determined by their crystal structures [2, 3, 5, 7]. Oxides with the general composition Ln_2TO_4 (where Ln is the rare earth element (REE), T is the 3*d* metal atom) with a layered structure formed of alternating blocks with perovskite and rock salt structures are promising cathode materials for solid-oxide fuel cells (SOFC). However, unlike nickelates Ln_2NiO_4, REE ferrites and cobaltites $Ln_2(Co,Fe)O_4$ do not form in air [8]. Partial substitution of alkaline-earth metals (AEM) for REE ions is accompanied by an increase in the average oxidation state of the 3*d* metal ions, resulting in the stabilization of the above structure [9-19]. Additional substitution in B-sublattice allows us to obtain materials with a high mixed electron-ion conductivity and acceptable thermal expansion coefficients [20-23].

Calcium-substituted samarium cobaltites $Sm_{2-x}Ca_xCoO_{4-\delta}$ exist at 1100 °C in air in a narrow composition range ($0.8 \le x \le 1.0$) [18]. The crystal structure of $SmCaCoO_{4-\delta}$ oxide is described with the tetragonal unit cell of the space group

Institute of Natural Sciences and Mathematics, Ural Federal University, Ekaterinburg, Russia; anastasia.galaida@urfu.ru. Original article submitted December 03, 2018; revised December 24, 2018; accepted December 25, 2018.

*I*4/*mmm*. A decrease in the calcium concentration in $Sm_{2-x}Ca_xCoO_{4-\delta}$ solid solutions ($x = 0.8$ and 0.9) is accompanied by a change in the crystal structure to orthorhombic (space group *Bmab*). Such a symmetry reduction with a change in the ratio between REEs and AEMs in A-sublattice has previously been noted for $Ln_{2-x}Ca_xCoO_{4\pm\delta}$ oxides with medium- and small-radius lanthanides (Sm, Eu, Gd) [19]. There is practically no literature data on the existence of substituted ferrites with the general composition $Ln_{2-x}Ca_xFeO_{4\pm\delta}$. It is known that when the temperature decreases to 1100 °C, $CaLaFeO_{4-\delta}$ complex oxide synthesized at atmospheric pressure and 1500 °C decomposes into lanthanum ferrite $LaFeO_{3-\delta}$ and calcium oxide CaO [24].

The work aims to determine the effect of cobalt and iron ion concentrations on the homogeneity ranges and the crystal structures of $SmCaCo_{1-x}Fe_xO_{4-\delta}$ and $Sm_{0.9}Ca_{1.1}Fe_{1-y}Co_yO_{4-\delta}$ solid solutions.

EXPERIMENTAL

The samples for the study were synthesized using the glycerol-nitrate technique. The following precursors were used to prepare the samples: samarium oxide Sm_2O_3 (SmO-L grade) and calcium carbonate $CaCO_3$ (analytical grade), which were preliminary annealed to remove adsorbed moisture and gases, metallic cobalt, iron oxalate $FeC_2O_4 \cdot 2H_2O$ (analytical grade), nitric acid HNO_3 (analytical grade) to dissolve the precursors, and glycerol (analytical grade) as a chelating agent and organic fuel for the reaction mixture pyrolysis. Metallic cobalt was obtained by reduction from Co_3O_4 oxide (high purity grade) at 500-600 °C in the hydrogen flow. The final annealing was carried out at 1100 °C in air for 120 h with intermediate grinding in the ethanol medium and subsequent slow cooling to room temperature.

The phase composition of the annealed samples was determined by powder X-ray diffraction. The phase composition of the samples was determined on an Equinox-3000 diffractometer (CuK_α radiation, in an angle range $2\theta = 10$-90° with a step of 0.012°). The phases were identified using the ICDD database and the Fpeak software package (Institute of Natural Sciences and Mathematics, Ural Federal University).

The structures of the samples under study were refined by the full-profile Rietveld method using the Fullprof 2008 software.

RESULTS AND DISCUSSION

$SmCaCo_{1-x}Fe_xO_{4-\delta}$ solid solutions. In order to investigate whether it is possible to obtain complex oxides with the general composition $SmCaCo_{1-x}Fe_xO_{4-\delta}$ using the glycerol-nitrate technique the samples with $0 \le x \le 0.5$ with a step $\Delta x = 0.1$ were synthesized. From the powder X-ray diffraction (XRD) data it is found that the homogeneity range of $SmCaCo_{1-x}Fe_xO_{4-\delta}$ solid solutions lies within $0 \le x \le 0.3$. The crystal structure of oxide with $x = 0.1$, which is similar to unsubstituted samarium cobaltite $SmCaCoO_{4-\delta}$ [18], is described with the tetragonal unit cell of the space group *I*4/*mmm*. A subsequent increase in the iron content ($x = 0.2$ and 0.3) results in the symmetry reduction to orthorhombic (space group *Bmab*). Fig. 1 depicts the X-ray diffraction patterns of $SmCaCo_{0.9}Fe_{0.1}O_{4-\delta}$ (*a*) and $SmCaCo_{0.7}Fe_{0.3}O_{4-\delta}$ (*b*) complex oxides refined by the full-profile Rietveld method.

For all single-phase $SmCaCo_{1-x}Fe_xO_{4-\delta}$ ($0 \le x \le 0.3$) samples the unit cell parameters and volumes, the atomic coordinates (Table 1), the average bond lengths and the angles between the metal–oxygen bonds (Table 2) were calculated from the X-ray diffraction data.

Both types of the structures are characterized by the statistical distribution of metal atoms in A and B sublattices. The 3*d* metal ions (Co^{n+}/Fe^{n+}) occupy the crystallographic site 2*a* (0, 0, 0). In the samples with the tetragonal structure, the samarium and calcium ions occupy the site 4*e* (0, 0, *z*), the oxygen ions (O1 and O2) occupy sites 4*c* (0, 1/2, 0) and 4*e* (0, 0, *z*). In the orthorhombic structure, cations (Sm^{3+}/Ca^{2+}) are displaced in the A sublattice along the crystallographic *y* axis relative to the respective sites in the tetragonal structure. The tilt of the oxygen octahedra (CoO_6) is accompanied by a displacement of O1 and O2 oxygen ions along the *z* and *y* axes respectively. Then, in the description of the crystal structure

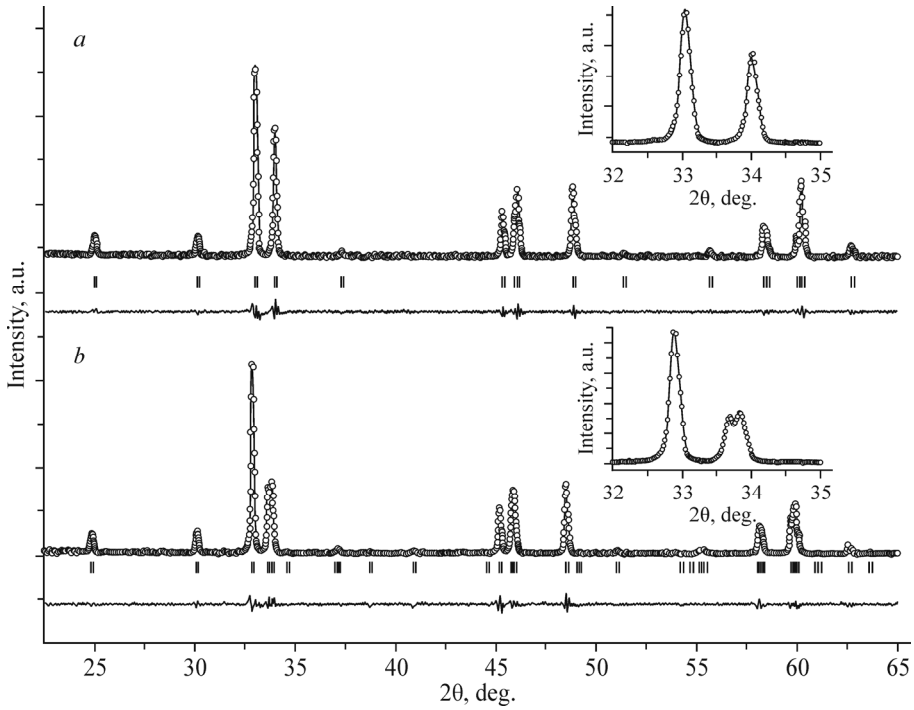

Fig. 1. X-ray diffraction data for $SmCaCo_{0.9}Fe_{0.1}O_{4-\delta}$ (*a*) and $SmCaCo_{0.7}Fe_{0.3}O_{4-\delta}$ (*b*) refined by the Rietveld method. Dots are the experimental data; the upper solid line is the theoretical profile; the lower solid line is the difference between the experimental data and the theoretical curve.

TABLE 1. Unit Cell Parameters and Atomic Coordinates for $SmCaCo_{1-x}Fe_xO_{4-\delta}$ ($0 \le x \le 0.3$) and $Sm_{0.9}Ca_{1.1}Fe_{1-y}Co_yO_{4-\delta}$ ($0 \le y \le 0.7$) Solid Solutions

Composition	Space group	*a*, Å	*b*, Å	*c*, Å	Sm / Ca		O1	O2		R_{Br},%	R_f,%
					y	*z*	*z*	*y*	*z*		
x = 0.0 [15]	*I*4/*mmm**	3.719(1)		11.873(1)	0.000(0)	0.358(1)	0.000(0)	0.000(0)	0.192(1)	–	–
x = 0.1		3.729(1)		11.854(1)	0.000(0)	0.360(1)	0.000(0)	0.000(0	0.170(0)	4.16	3.14
x = 0.2	*Bmab*	5.286(1)	5.305(1)	11.861(1)	–0.004(1)	0.361(1)	–0.005(1)	0.049(1)	0.171(1)	5.90	7.14
x = 0.3		5.297(1)	5.323(1)	11.875(1)	–0.004(1)	0.361(1)	–0.008(1)	0.056(1)	0.170(1)	4.34	5.84
y = 0.0		5.390(1)	5.452(1)	12.039(1)	–0.016(1)	0.356(1)	–0.018(1)	0.058(1)	0.174(1)	6.97	6.97
y = 0.1		5.378(1)	5.443(1)	11.982(1)	–0.011(1)	0.358(1)	–0.015(1)	0.062(1)	0.169(1)	4.75	5.79
y = 0.2		5.359(1)	5.420(1)	11.963(1)	–0.001(1)	0.358(1)	–0.015(1)	0.058(1)	0.172(1)	5.41	6.57
y = 0.3		5.338(1)	5.388(1)	11.948(1)	0.006(1)	0.358(1)	–0.015(1)	0.009(1)	0.171(1)	4.09	8.42
y = 0.4		5.344(1)	5.400(1)	11.942(1)	–0.008(1)	0.358(1)	–0.019(1)	0.054(1)	0.173(1)	7.41	7.41
y = 0.5		5.331(1)	5.379(1)	11.927(1)	–0.008(1)	0.359(1)	–0.018(1)	0.050(1)	0.173(1)	7.12	7.43
y = 0.6		5.302(1)	5.332(1)	11.901(1)	–0.006(1)	0.359(1)	–0.012(1)	0.037(1)	0.174(1)	6.81	6.81
y = 0.7	*I*4/*mmm*	3.748(1)		11.889(1)	0.000(0)	0.359(1)	0.000(0)	0.000(0)	0.173(1)	4.51	3.21

* The atomic sites for the space group *I*4/*mmm*: Sm/Ca (0, 0, *z*); Co/Fe (0, 0, 0); O1 (0.5, 0, 0); O2 (0, 0, *z*); space group *Bmab*: Sm/Ca (0, *y*, *z*); Co/Fe (0, 0, 0); O1 (0.25, 0.25, *z*); O2 (0, *y*, *z*).

of the samples the $\sqrt{2}\,a_p \times \sqrt{2}\,a_p \times c$ unit cell should be used, where a_p is the unit cell parameter of the ideal cubic perovskite; *c* corresponds to the *c* unit cell parameter of the tetragonal phase of the K_2NiF_4 type. Fig. 2 shows the models of unit cells of complex oxides with tetragonal (*a*) and orthorhombic (*b*) structures constructed using the Diamond software.

TABLE 2. Average Bond Lengths and Angles Between the Metal–Oxygen Bondsin $SmCaCo_{1-x}Fe_xO_{4-\delta}$ ($0 \le x \le 0.3$) and $Sm_{0.9}Ca_{1.1}Fe_{1-y}Co_yO_{4-\delta}$ ($0 \le y \le 0.7$)

Composition	A–O1, Å	B–O1, Å	A–O2, Å	B–O2, Å	O1–B–O1, deg	O1–B–O2, deg
$x = 0.0$	2.484(2)	1.857(1)	2.284(2)	1.999(2)	90(0)	90(0)
$x = 0.1$	2.492(1)	1.864(1)	2.261(5)	2.011(2)	90(0)	90(0)
$x = 0.2$	2.502(1)	1.881(1)	2.593(2)	2.017(1)	89.7(1)	93.3(1)
$x = 0.3$	2.515(1)	1.884(1)	2.593(2)	2.047(2)	89.8(1)	91.9(1)
$y = 0.0$	2.586(2)	1.929(2)	2.634(1)	2.103(1)	88.6(1)	91.8(1)
$y = 0.1$	2.566(1)	1.921(1)	2.643(2)	2.020(2)	88.8(1)	90.6(1)
$y = 0.2$	2.555(1)	1.910(1)	2.702(1)	2.052(2)	89.1(1)	90.7(1)
$y = 0.3$	2.546(2)	1.905(2)	2.610(3)	2.049(2)	90.0(1)	94.4(1)
$y = 0.4$	2.550(1)	1.909(1)	2.614(1)	2.074(1)	90.0(1)	93.5(1)
$y = 0.5$	2.485(1)	1.903(2)	2.608(1)	2.081(2)	89.9(1)	92.4(1)
$y = 0.6$	2.520(2)	1.886(1)	2.596(1)	2.083(2)	89.9(1)	91.4(1)
$y = 0.7$	2.509(2)	1.874(2)	2.672(2)	2.017(1)	90(0)	90(0)

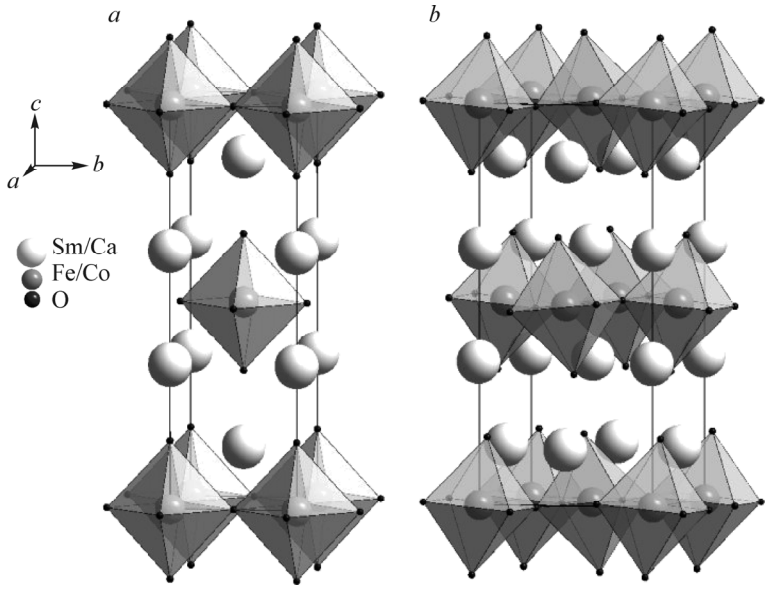

Fig. 2. Model of the unit cell of complex oxides with tetragonal (*a*) and orthorhombic (*b*) structures.

It is found that an increase in the concentration of iron ions in the $SmCaCo_{1-x}Fe_xO_{4-\delta}$ solid solution results in an increase in the unit cell parameters and volume due to a large iron ion radius as compared to the cobalt ion (for the octahedral environment $r_{HS/LS}(Fe^{3+}) = 0.645/0.55$ Å, $r_{HS/LS}(Co^{3+}) = 0.61/0.545$ Å [25]).

In accordance with Vegard's rule, the concentration dependence of the unit cell volume for the $SmCaCo_{1-x}Fe_xO_{4-\delta}$ samples is linear (Fig. 3). For comparison, the unit cell volumes of the samples with the orthorhombic structure are reduced to the tetragonal unit cell volume.

$Sm_{0.9}Ca_{1.1}Fe_{1-y}Co_yO_{4-\delta}$ solid solutions. According to the powder XRD data, samarium-calcium ferrite $Sm_{0.9}Ca_{1.1}FeO_{4-\delta}$ crystallizes in the orthorhombic unit cell of the space group *Bmab*. Cobalt doping of $Sm_{0.9}Ca_{1.1}FeO_{4-\delta}$ ferrite in the B sublattice results in the formation of several $Sm_{0.9}Ca_{1.1}Fe_{1-y}Co_yO_{4-\delta}$ solid solutions with $0 \le y \le 0.7$. The X-ray diffraction patterns of the samples with $0.1 \le y \le 0.6$ are described with the orthorhombic perovskite-like unit cell of the space group *Bmab*, while complex oxide with the cobalt content $y = 0.7$ has the tetragonal structure (space group *I*4/*mmm*).

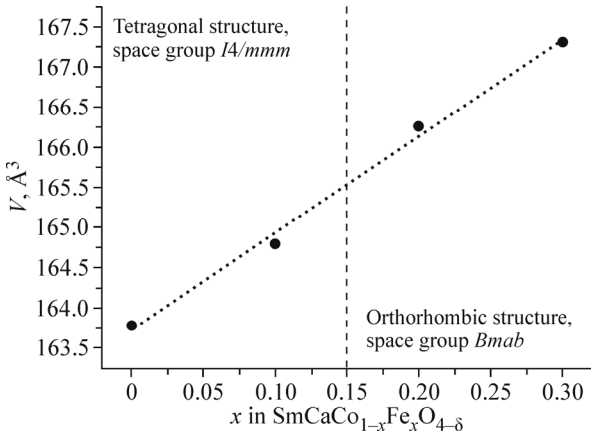

Fig. 3. Dependence of the unit cell volume of the $SmCaCo_{1-x}Fe_xO_{4-\delta}$ solid solution on the concentration of iron ions.

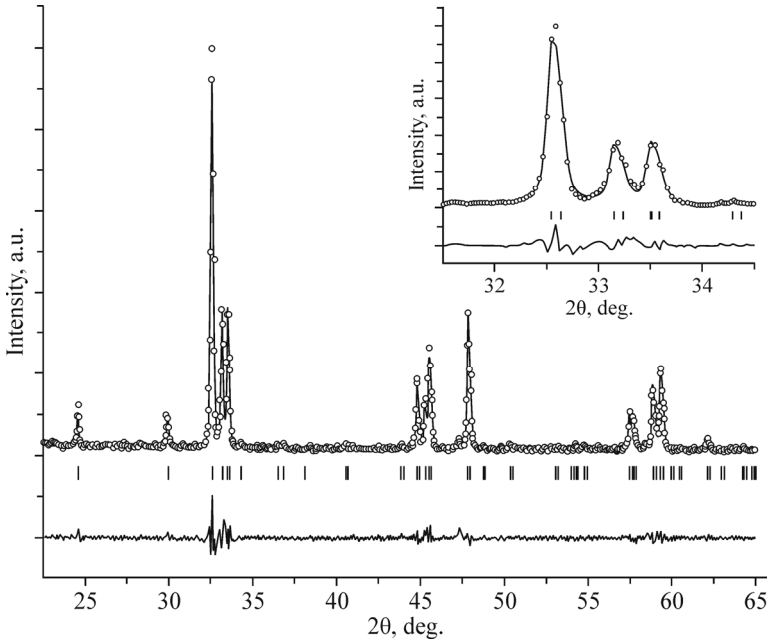

Fig. 4. X-ray diffraction data for $Sm_{0.9}Ca_{1.1}Fe_{0.6}Co_{0.4}O_{4-\delta}$ refined by the Rietveld method.

Fig. 4 depicts the X-ray diffraction pattern of $Sm_{0.9}Ca_{1.1}Fe_{0.6}Co_{0.4}O_{4-\delta}$ complex oxide refined by the full-profile Rietveld method.

For all single-phase $Sm_{0.9}Ca_{1.1}Fe_{1-y}Co_yO_{4-\delta}$ oxides the structural parameters were calculated (Tables 1 and 2). With an increase in the cobalt concentration in the samples the parameters monotonically decrease, which can be explained in terms of size effects. The concentration dependences of the $Sm_{0.9}Ca_{1.1}Fe_{1-y}Co_yO_{4-\delta}$ unit cell parameters are given in Fig. 5.

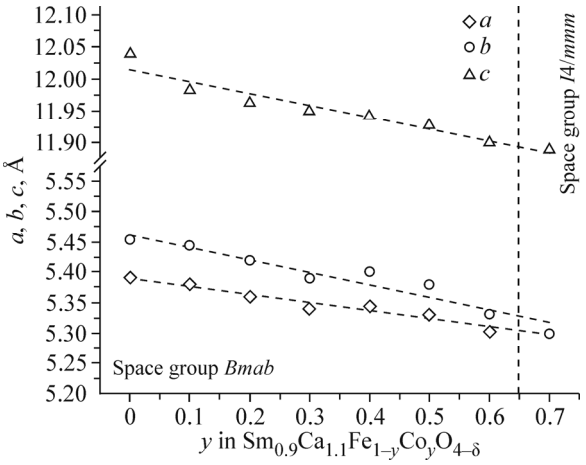

Fig. 5. Dependence of the unit cell volume of the $Sm_{0.9}Ca_{1.1}Fe_{1-y}Co_yO_{4-\delta}$ solid solution on the concentration of cobalt ions.

CONCLUSIONS

The $SmCaCo_{1-x}Fe_xO_{4-\delta}$ ($0 \le x \le 0.5$) and $Sm_{0.9}Ca_{1.1}Fe_{1-y}Co_yO_{4-\delta}$ ($0.0 \le y \le 0.7$) solid solutions were synthesized using the glycerol-nitrate technique at 1100 °C in air. It is established that the REE/AEM ratio in the A sublattice and the Fe/Co ratio in the B sublattice substantially affect the crystal structures of the samples: $SmCaCo_{1-x}Fe_xO_{4-\delta}$ and $Sm_{0.9}Ca_{1.1}Fe_{1-y}Co_yO_{4-\delta}$ solid solutions enriched by cobalt crystallized in the tetragonal unit cell and the samples with a high concentration of iron ions crystallized in the orthorhombic unit cell. An increase in the iron ion content in the samples results in a monotonic increase in the unit cell parameters and volume of the samples.

CONFLICT OF INTERESTS

The authors declare that they have no conflict of interests.

REFERENCES

1. A. Petric, P. Huang, and F. Tietz. *Solid State Ion*., **2000**, *135*, 719.
2. S. Ya. Istomin and E. V. Antipov. *Russ. Chem. Rev*., **2013**, *82*, 686.
3. J. Dailly, S. Fourcade, A. Largeteau, F. Mauvy, J. C. Grenier, and M. Marrony. *Electrochim. Acta*, **2010**, *55*, 5847.
4. Sh. I. Elkalashy, A. R. Gilev, T. V. Aksenova, A. S. Urusova, and V. A. Cherepanov. *Solid State Ion*., **2018**, *316*, 85.
5. M. Al Daroukh, V. V. Vashook, H. Ullmann, F. Tietz, and I. Arual Raj. *Solid State Ion*., **2003**, *158*, 141.
6. V. V. Kharton, E. V. Tsipis, A. A. Yaremchenko, and J. R. Frade. *Solid State Ion*., **2004**, *166*, 327.
7. F. Zhao, X. Wang, Z. Wang, R. Peng, and C. Xia. *Solid State Ion*., **2008**, *179*, 1450.
8. A. N. Petrov, V. A. Cherepanov, A. Yu. Zuyev, and V. M. Zhukovsky. *J. Solid State Chem*., **1988**, *77*, 1.
9. H. Taguchi, H. Kido, and T. Tabata. *Physica B*, **2004**, *344*, 271.
10. H. Taguchi, K. Nakade, and K. Hirota. *Mater. Res. Bull*., **2007**, *42*, 649.
11. W. Wong-Ng, W. Laws, K. R. Talley, Q. Huang, Y. Yan, J. Martin, and J. A. Kaduk. *J. Solid State Chem*., **2014**, *215*, 128.
12. W. Wong-Ng, W. Laws, S. H. Lapidus, L. Ribaud, and J. A. Kaduk. *Solid State Sci*., **2017**, *72*, 47.
13. W. Wong-Ng, W. Laws, and J. A. Kaduk. *Solid State Sci*., **2016**, *58*, 105.
14. W. Wong-Ng, W. Laws, S. H. Lapidus, and J. A. Kaduk. *Solid State Sci*., **2015**, *48*, 31.
15. N. E. Volkova, A. V. Maklakova, L. Ya. Gavrilova, and V. A. Cherepanov. *Eur. J. Inorg. Chem*., **2017**, 3285.

16. O. A. Shlyakhtin, G. N. Mazo, M. S. Kaluzhskikh, D. A. Komissarenko, A. S. Loktev, and A. G. Dedov. *Mater. Lett*., **2012**, *75*, 20.
17. V. A. Cherepanov, L. Ya. Gavrilova, L. Yu. Barkhatova, V. I. Voronin, M. V. Trifonova, and O. A. Bukhner. *Ionics*, **1998**, *4*, 309.
18. A. P. Galayda, N. E. Volkova, L. Ya. Gavrilova, K. G. Balymov, and V. A. Cherepanov. *J. Alloys Compd*., **2017**, *718*, 288.
19. G. J. Thorogood, P.-Y. Orain, M. Ouvry, B. Piriou, T. Tedesco, K. S. Wallwork, J. Herrmann, and M. James. *J. Solid State Chem*., **2011**, *13*, 2113.
20. L.-W. Tai, M. M. Nasrallah, H. U. Anderson, D. M. Sparlin, and S. R. Sehlin. *Solid State Ion*., **1995**, *76*, 259.
21. S. Ki-Woog and L. Ki-Tae. *Ceram. Int*., **2011**, *37*, 573.
22. K. T. Lee and A. Manthiram. *Solid State Ion*., **2005**, *176*, 1521.
23. A. Petric, P. Huang, and F. Tietz. *Solid State Ion*., **2000**, *135*, 719.
24. M. M. Nguyen-Trut-Dinh, M. Vlasse, M. Perrin, and G. Le Flem. *J. Solid State Chem*., **1980**, *32*, 1.
25. R. D. Shannon. *Acta Crystallogr*., **1976**, *32*, 751.